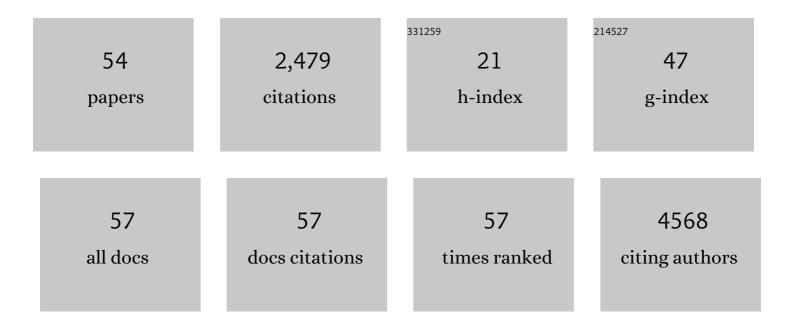
## Anna Tietze

List of Publications by Year in descending order

Source: https://exaly.com/author-pdf/3641623/publications.pdf Version: 2024-02-01



#	Article	IF	CITATIONS
1	Tumor load rather than contrast enhancement is associated with the visual function of children and adolescents with optic pathway glioma – a retrospective Magnetic Resonance Imaging study. Journal of Neuro-Oncology, 2022, 156, 589-597.	1.4	7
2	ls cannabidiol worth a trial in Rasmussen encephalitis?. European Journal of Paediatric Neurology, 2022, 37, 53-55.	0.7	3
3	Epilepsy surgery in the first six months of life: A systematic review and meta-analysis. Seizure: the Journal of the British Epilepsy Association, 2022, 96, 109-117.	0.9	12
4	Personalizing Deep Brain Stimulation Using Advanced Imaging Sequences. Annals of Neurology, 2022, 91, 613-628.	2.8	22
5	Assessment of myelination in infants and young children by T1 relaxation time measurements using the magnetization-prepared 2 rapid acquisition gradient echoes sequence. Pediatric Radiology, 2021, 51, 2058-2068.	1.1	9
6	Infratentorial MRI Findings in Rasmussen Encephalitis Suggest Primary Cerebellar Involvement. Neurology: Neuroimmunology and NeuroInflammation, 2021, 8, .	3.1	4
7	Cerebral Macro- and Microcirculation during Ephedrine versus Phenylephrine Treatment in Anesthetized Brain Tumor Patients: A Randomized Clinical Trial Using Magnetic Resonance Imaging. Anesthesiology, 2021, 135, 788-803.	1.3	20
8	Case Report: Hemispherotomy in the First Days of Life to Treat Drug-Resistant Lesional Epilepsy. Frontiers in Neurology, 2021, 12, 818972.	1.1	6
9	Impaired perfusion and capillary dysfunction in prodromal Alzheimer's disease. Alzheimer's and Dementia: Diagnosis, Assessment and Disease Monitoring, 2020, 12, e12032.	1.2	18
10	Crediting multi-authored papers to single authors. Physica A: Statistical Mechanics and Its Applications, 2020, 554, 124652.	1.2	4
11	Classification of Intracranial Stenoses: Discrepancies between Transcranial Duplex Sonography and Computed Tomography Angiography. Ultrasound in Medicine and Biology, 2020, 46, 1889-1895.	0.7	6
12	Ephedrine <i>versus</i> Phenylephrine Effect on Cerebral Blood Flow and Oxygen Consumption in Anesthetized Brain Tumor Patients. Anesthesiology, 2020, 133, 304-317.	1.3	30
13	Abnormal Amyloid Load in Mild Cognitive Impairment: The Effect of Reducing the PiBâ€₽ET Threshold. Journal of Neuroimaging, 2019, 29, 499-505.	1.0	13
14	Dynamic cerebellar herniation in Chiari patients during the cardiac cycle evaluated by dynamic magnetic resonance imaging. Neuroradiology, 2019, 61, 825-832.	1.1	4
15	The h-index and multi-author hm-index for individual researchers in condensed matter physics. Scientometrics, 2019, 119, 171-185.	1.6	8
16	Lead-DBS v2: Towards a comprehensive pipeline for deep brain stimulation imaging. NeuroImage, 2019, 184, 293-316.	2.1	527
17	Robust estimation of hemo-dynamic parameters in traditional DCE-MRI models. PLoS ONE, 2019, 14, e0209891.	1.1	6
18	Prediction of Tissue Outcome and Assessment of Treatment Effect in Acute Ischemic Stroke Using Deep Learning. Stroke, 2018, 49, 1394-1401.	1.0	156

Anna Tietze

#	Article	IF	CITATIONS
19	Comparison of single and dual energy CT for stopping power determination in proton therapy of head and neck cancer. Physics and Imaging in Radiation Oncology, 2018, 6, 14-19.	1.2	28
20	The role of computed tomography in the screening of patients presenting with symptoms of an intracranial tumour. Acta Neurochirurgica, 2018, 160, 667-672.	0.9	2
21	Noninvasive assessment of isocitrate dehydrogenase mutation status in cerebral gliomas by magnetic resonance spectroscopy in a clinical setting. Journal of Neurosurgery, 2018, 128, 391-398.	0.9	62
22	Diffusion MRI findings in patients with extensive and minimal post-concussion symptoms after mTBI and healthy controls: a cross sectional study. Brain Injury, 2018, 32, 91-98.	0.6	9
23	Bayesian modeling of Dynamic Contrast Enhanced MRI data in cerebral glioma patients improves the diagnostic quality of hemodynamic parameter maps. PLoS ONE, 2018, 13, e0202906.	1.1	9
24	Molecularly defined diffuse leptomeningeal glioneuronal tumor (DLGNT) comprises two subgroups with distinct clinical and genetic features. Acta Neuropathologica, 2018, 136, 239-253.	3.9	118
25	Microstructural changes in the thalamus after mild traumatic brain injury: A longitudinal diffusion and mean kurtosis tensor MRI study. Brain Injury, 2017, 31, 230-236.	0.6	33
26	Reliable estimation of microvascular flow patterns in patients with disrupted blood–brain barrier using dynamic susceptibility contrast MRI. Journal of Magnetic Resonance Imaging, 2017, 46, 537-549.	1.9	13
27	Brain inflammation accompanies amyloid in the majority of mild cognitive impairment cases due to Alzheimer's disease. Brain, 2017, 140, 2002-2011.	3.7	147
28	Effect of ephedrine and phenylephrine on brain oxygenation and microcirculation in anaesthetised patients with cerebral tumours: study protocol for a randomised controlled trial. BMJ Open, 2017, 7, e018560.	0.8	4
29	Automatic thalamus and hippocampus segmentation from MP2RAGE: comparison of publicly available methods and implications for DTI quantification. International Journal of Computer Assisted Radiology and Surgery, 2016, 11, 1979-1991.	1.7	40
30	Perfusion and pH MRI in familial hemiplegic migraine with prolonged aura. Cephalalgia, 2016, 36, 279-283.	1.8	17
31	Microcirculatory dysfunction and tissue oxygenation in critical illness. Acta Anaesthesiologica Scandinavica, 2015, 59, 1246-1259.	0.7	48
32	Accuracy of 18F-FDG PET-CT in triaging lung cancer patients with suspected brain metastases for MRI. Nuclear Medicine Communications, 2015, 36, 1084-1090.	0.5	17
33	Perfusion MRI Derived Indices of Microvascular Shunting and Flow Control Correlate with Tumor Grade and Outcome in Patients with Cerebral Glioma. PLoS ONE, 2015, 10, e0123044.	1.1	34
34	The impact of reliable prebolus T 1 measurements or a fixed T 1 value in the assessment of glioma patients with dynamic contrast enhancing MRI. Neuroradiology, 2015, 57, 561-572.	1.1	21
35	Biased visualization of hypoperfused tissue by computed tomography due to short imaging duration: improved classification by image down-sampling and vascular models. European Radiology, 2015, 25, 2080-2088.	2.3	3
36	Spatial distribution of malignant tissue in gliomas: correlations of <sup>11</sup> C-L-methionine positron emission tomography and perfusion- and diffusion-weighted magnetic resonance imaging. Acta Radiologica, 2015, 56, 1135-1144.	0.5	19

Anna Tietze

#	Article	IF	CITATIONS
37	Mean Diffusional Kurtosis in Patients with Glioma: Initial Results with a Fast Imaging Method in a Clinical Setting. American Journal of Neuroradiology, 2015, 36, 1472-1478.	1.2	70
38	Pseudoprogression after proton radiotherapy for pediatric low grade glioma. Acta Oncológica, 2015, 54, 1701-1702.	0.8	9
39	Patch-Based Segmentation from MP2RAGE Images: Comparison to Conventional Techniques. Lecture Notes in Computer Science, 2015, , 180-187.	1.0	2
40	Capillary Transit Time Heterogeneity and Flow-Metabolism Coupling after Traumatic Brain Injury. Journal of Cerebral Blood Flow and Metabolism, 2014, 34, 1585-1598.	2.4	114
41	Assessment of ischemic penumbra in patients with hyperacute stroke using amide proton transfer (APT) chemical exchange saturation transfer (CEST) MRI. NMR in Biomedicine, 2014, 27, 163-174.	1.6	144
42	Dabigatran-related Intracerebral Hemorrhage Resulting in Hematoma Expansion. Journal of Stroke and Cerebrovascular Diseases, 2014, 23, e133-e134.	0.7	18
43	Effect of thyroxine on brain microstructure in extremely premature babies: magnetic resonance imaging findings in the TIPIT study. Pediatric Radiology, 2014, 44, 987-996.	1.1	11
44	The Role of the Microcirculation in Delayed Cerebral Ischemia and Chronic Degenerative Changes after Subarachnoid Hemorrhage. Journal of Cerebral Blood Flow and Metabolism, 2013, 33, 1825-1837.	2.4	140
45	The Relationship between Tumor Blood Flow, Angiogenesis, Tumor Hypoxia, and Aerobic Glycolysis. Cancer Research, 2013, 73, 5618-5624.	0.4	140
46	The Role of the Cerebral Capillaries in Acute Ischemic Stroke: The Extended Penumbra Model. Journal of Cerebral Blood Flow and Metabolism, 2013, 33, 635-648.	2.4	115
47	Paraplegia due to drop metastases from anaplastic oligodendroglioma. British Journal of Neurosurgery, 2012, 26, 94-95.	0.4	8
48	Prophylactic cranial irradiation in patients with small cell lung cancer. A retrospective study of recurrence, survival and morbidity. Lung Cancer, 2012, 77, 561-566.	0.9	24
49	Changes in 3-dimensional bone structure indices in hypoparathyroid patients treated with PTH(1-84): A randomized controlled study. Journal of Bone and Mineral Research, 2012, 27, 781-788.	3.1	67
50	Left–right difference in fetal liver oxygenation during hypoxia estimated by BOLD MRI in a fetal sheep model. Ultrasound in Obstetrics and Gynecology, 2011, 38, 665-672.	0.9	14
51	Reduced Prediagnostic 25-Hydroxyvitamin D Levels in Women with Breast Cancer: A Nested Case-Control Study. Cancer Epidemiology Biomarkers and Prevention, 2009, 18, 2655-2660.	1.1	57
52	BOLD MRI in sheep fetuses: a nonâ€invasive method for measuring changes in tissue oxygenation. Ultrasound in Obstetrics and Gynecology, 2009, 34, 687-692.	0.9	43
53	TIPIT: A randomised controlled trial of thyroxine in preterm infants under 28 weeks gestation: Magnetic Resonance Imaging and Magnetic Resonance Angiography protocol. BMC Pediatrics, 2008, 8, 26.	0.7	4
54	Acute myeloid and Tâ€cell acute lymphoblastic leukaemia with aberrant antigen expression exhibit similar TCRδ gene rearrangements. British Journal of Haematology, 1996, 92, 929-936.	1.2	18